(11) "Gmelins Handbuch der Anorganischen Chemie," Iron 59B, Verlag Chemie, GmbH, Berlin, 1938.
(12) K. Nakamoto, "Infrared Spectra of Inorganic and Coordination Compounds," Wiley, New York, N.Y., 1963.
(13) J. H. Swinehart and P. A. Rock, *Inorg. Chem.*, **5**, 573 (1966).
(14) J. Bjerrum, G. Schwarzenbach, and L. G. Sillén, *Chem. Soc., Spec. Publ.*, **No. 7**, 53 (1958).
(15) Q. H. Gibson and F. J. W. Roughton, *J. Physiol. (London)*, **136**, 507 (1957).
(16) S. K. Wolfe, C. Andrade, and J. H. Swinehart, *Inorg. Chem.*, **13**, 2567 (1974).
(17) W. L. Jolly, "The Inorganic Chemistry of Nitrogen," W. A. Benjamin, New York, N.Y., 1964.
(18) M. Anbar and H. Taube, *J. Amer. Chem. Soc.*, **76**, 6243 (1954).
(19) A. Haim and H. Taube, *Inorg. Chem.*, **2**, 1199 (1963).
(20) This is nearly identical with the result calculable for diffusion-controlled rates from the modified Debye equation [H. L. J. Bäckstrom and K. Sandros, *Acta Chem. Scand.*, **14**, 48 (1960)]: $k_{\mathrm{diff}} = {}^1/_4[2 + (d_1/d_2) + (d_2/d_1)](8RT/3 \times 10^3\eta)$, where k_{diff} is in M^{-1} sec^{-1}, η is the viscosity of the solvent (8.94×10^{-3} g sec^{-1} cm^{-1} for water at 25°), $R = 8.31 \times 10^7$ ergs M^{-1} deg^{-1}, and d_1 and d_2 are the (assumed spherical) diameters of the reactants. For simplicity, assuming $d_1 = d_2$ (a difference of 50% in diameters only affects the calculated rate constant by *ca.* 5%), $k_{\mathrm{diff}} = 0.7 \times 10^{10}$ M^{-1} sec^{-1} (25°).
(21) J. H. Swinehart, *Coord. Chem. Rev.*, **2**, 385 (1967).
(22) M. M. Wendel and R. L. Pigford, *AIChE J.*, **4**, 249 (1958).
(23) D. M. Yost and H. R. Russell, "Systematic Inorganic Chemistry," Prentice-Hall, Englewood Cliffs, N.J., 1946.
(24) Oxygen is consumed at a continuous proportion of ${}^1/_3$ mol/mol of nitrous acid formed. Then the total oxygen consumption, $S_{\mathrm{O_2}}$, per mole of nitroprusside photolyzed is given by the expression $S_{\mathrm{O_2}} = {}^1/_2\sum_{n=0}^{\infty}({}^1/_3)^n$. The sum of this series can be calculated from $S = a[(1 - r^n)/(1 - r)]$, where a is the first term of the series, ${}^1/_2$; r^n the last term, approaching zero; and r is the common ratio, ${}^1/_3$. Substitution gives $S_{\mathrm{O_2}} = 0.75$.
(25) "Standard Methods of Chemical Analysis," Vol. 2, Part B, 6th ed, Van Nostrand, New York, N.Y., 1963.
(26) I. Crivelli and C. Andrade, personal communication, 1970.
(27) S. K. Wolfe and J. H. Swinehart, unpublished results, 1970.
(28) R. F. Fenske and R. L. DeKock, *Inorg. Chem.*, **11**, 437 (1972).
(29) P. T. Manoharan and H. B. Gray, *Inorg. Chem.*, **5**, 823 (1966).
(30) V. Balzani and V. Carassiti, "Photochemistry of Coordination Compounds," Academic Press, New York, N.Y., 1970.

Contribution from the Metcalf Research Laboratory,
Department of Chemistry, Brown University, Providence, Rhode Island 02912

Spectroscopic Studies of Metal–Metal Bonding. VII. Absorption and Laser Raman Spectra and Vibrational Analyses of $[(OC)_5Re-M'(CO)_5]^-$ (M' = Cr, Mo, W)

JOHN R. JOHNSON,[1] D. MICHAEL DUGGAN, and WILLIAM M. RISEN, Jr.*

Received October 4, 1974 AIC40691M

The absorption spectra (33–35,000 cm^{-1}) for the metal–metal bonded species $ReCr(CO)_{10}^-$, $ReMo(CO)_{10}^-$, and $ReW(CO)_{10}^-$ and the results of laser Raman measurements (0–2200 cm^{-1}), where obtainable, are reported. The vibrational spectral features have been assigned on the basis of C_{4v} symmetry, normal-coordinate analyses based on these assignments have been performed, and k(Re–M') values have been found to be in the order k(Re–W) > k(Re–Mo) > k(Re–Cr). For isoelectronic species k(Re–Re) > k(Re–W) and k(Re–Mn) > k(W–Mn) > k(Re–Cr). Comparison of "k(M–M')" values of the $ReM'(CO)_{10}^-$ anions, of the previously investigated $MnM'(CO)_{10}^-$ species, and of the neutral decacarbonyls $MM'(CO)_{10}$ (M = M' = Mn, Re, Tc; M = Mn; M' = Re) is made.

Introduction

The compounds $[(CO)_5Re-M'(CO)_5]^-$ (M' = Cr, Mo, W) are members of the $MM'(CO)_{10}$ series of metal–metal bonded molecules in which changes in metal–metal bond strength, k(M–M'), can be studied as a function of both M and M'. The complete series of known species includes $M_2(CO)_{10}$ (M = Mn, Tc, Re), $MM'(CO)_{10}$ (M = Mn; M' = Re), $MM'(CO)_{10}^-$ (M = Mn, Re; M' = Cr, Mo, W), and $M_2(CO)_{10}^{2-}$ (M = Cr, Mo, W). Each of these is essentially isostructural with the others, and isoelectronic relationships exist between individual species to form three series: (1) $Mn_2(CO)_{10}$, $MnCr(CO)_{10}^-$, and $Cr_2(CO)_{10}^{2-}$; (2) $Re_2(CO)_{10}$, $ReW(CO)_{10}^-$, and $W_2(CO)_{10}^{2-}$; (3) $ReMn(CO)_{10}$, $MnW(CO)_{10}^-$, and $ReCr(CO)_{10}^-$. To investigate series 2 and 3, the values of k(M–M') for $ReCr(CO)_{10}^-$ and $ReW(CO)_{10}^-$ are required, and to investigate the effect on k(M–M') of changing M' from a first- to second- to third-row transition metal bound to the same M, the complete $ReM'(CO)_{10}^-$ series is of interest. With reported studies of $MnM'(CO)_{10}^-$ [2] and $M_2(CO)_{10}$[3-15] series and $MnRe(CO)_{10}$,[4] this study of $ReM'(CO)_{10}^-$ series permits investigation of nuclear charge distribution effects on k(M–M') through isoelectronic series 2 and 3 above.

We report in this paper the infrared, laser Raman, and uv–visible spectra of the tetraethylammonium (Et_4N^+) salts of $ReCr(CO)_{10}^-$, $ReMo(CO)_{10}^-$, and $ReW(CO)_{10}^-$ and the tetraphenylarsonium (Ph_4As^+) salt of $ReW(CO)_{10}^-$, their vibrational normal-coordinate analyses, and the bonding implications of the results in comparison with the related species discussed above.

Experimental Section

The compounds $Et_4NReCr(CO)_{10}$, $Et_4NReMo(CO)_{10}$, $Et_4NReW(CO)_{10}$, and $Ph_4AsReW(CO)_{10}$ were prepared by the procedure of Anders and Graham[16] using modifications described previously.[2] The reagents were purified by sublimation, recrystallization, and distillation, where appropriate, and the reactions were carried out under dry N_2 or Ar. Samples of the compounds were prepared by recrystallization from 95% ethanol or by repeated recrystallization from tetrahydrofuran using *n*-pentane as the precipitating agent. The purity of each compound was established by elemental analyses (Re, M', C, H, N) and by the 5-μ infrared solution spectra. The analyses, performed by Baron Consulting Co. and Midwest Microlab, Inc., agreed with expected values to within 0.5% for the transition metals and 0.2% for C, H, and N. The 5-μ spectral measurements agreed with those of reported work.[16]

Solutions, mulls, powders, and pellets used for spectroscopic measurements were prepared and handled under a dry N_2 atmosphere or *in vacuo* using dried and deaerated solvents and were sealed in N_2-purged cells. Sealed capillary, fused-silica, and multipass Raman cells or sealed KBr, CsI, and high-density polyethylene far-infrared liquid cells were used where appropriate.

Infrared spectra were measured on a Beckman IR-11 or IR-12 spectrometer with a resolution and accuracy of *ca.* 1 cm^{-1} as determined by standard resolution tests and wave number calibration.[17] The mercury lamp (ir) source was filtered with carbon-filled polyethylene when used. The laser Raman spectra were measured on a Jarrell-Ash 25-300 Raman spectrometer, using He–Ne 632.8-nm laser radiation, with a resolution of *ca.* 3 cm^{-1} and an accuracy of 1 cm^{-1}. Uv–visible spectra were measured on a Cary 15 spectrometer.

Since these compounds are unstable in air and upon standing in solution, their 5-μ infrared spectra were recorded before, after, and from time to time during the measurement of the reported spectra, and spectra reported were reproduced several times on each of several different samples.

Spectral Results and Assignments

The molecular symmetry of the $ReM'(CO)_{10}^-$ anions is assumed to be C_{4v} by analogy to the known structures of the neutral decacarbonyls $M_2(CO)_{10}$ (M = Mn, Tc, Re)[18-20] and the dianionic species $M_2(CO)_{10}^{2-}$ (M = Cr, Mo).[21] In this structure four nearly coplanar carbonyl ligands are situated around each transition metal at 90° with the group of carbonyls on M rotated through an angle of 45° with respect to the group of carbonyls on Re. The observation of six infrared- and eight Raman-active fundamentals in the 5-μ (ν(CO)) spectral region, as predicted for each of these compounds, is evidence of the C_{4v} molecular symmetry.

Metal–metal bond lengths used in the vibrational calculations were estimated from the $M_2(CO)_{10}$ and $M_2(CO)_{10}^{2-}$ crystal structures[18-21] and consideration of the single-bond radii and oxidation states of the metals involved. The Re–Cr distance was taken as 2.98 Å and those used for the Re–Mo and Re–W compounds were taken to be 3.00 and 3.02 Å, respectively.[22] The M–C and C–O distances also were obtained from the crystal structures mentioned above and from those of hexacarbonyls $M(CO)_6$ (M = Cr, Mo, W).[23,24] All angles were taken to be 90 or 180°, in conformation with the idealized C_{4v} symmetry.

The vibrational representation for these compounds in C_{4v} symmetry is Γ_{VIB} = 13 A_1 (ir, Raman, pol) + 3 A_2 (ia) + 6 B_1 (Raman, depol) + 6 B_2 (Raman, depol) + 16 E (ir, Raman, depol). Observed fundamentals, their symmetries and depolarization ratios, and a partial description of the motions involved are given in Table I. A more extended tabulation of all observed bands, including their intensities, sample physical states, polarizations, and assignments, is available.[25]

It is convenient to discuss the observed infrared and Raman spectra for these compounds in three distinct regions: 5 μ (1800–2200 cm^{-1}), in which ν(C–O) motions occur; 300–800 cm^{-1}, in which ν(M–C) and δ(M–C–O) motions occur; 30–300 cm^{-1}, in which ν(M–M') motions and several types of skeletal deformations occur.

Spectra in the Region 1800–2200 cm^{-1}. Six infrared (4 A_1 + 2 E) and eight Raman (4 A_1 + 2 E + B_1 + B_2) ν(CO) fundamentals are expected in this region. As a convenient first approximation, half of these infrared- and Raman-active 5-μ fundamentals result from the $M'(CO)_5$ portion of a molecule with the remaining half arising from motion on the $Re(CO)_5$ moiety. There are two sets of CO ligands for each $M(CO)_5$ portion of a molecule: the four CO planar ligands around M' or Re plus the CO ligand along the C_4 axis. Three infrared (2 A_1 + E) and four Raman (2 A_1 + E + B) carbonyl stretching modes arise on an $M(CO)_5$ portion of each molecule. The 2 A_1 modes describe C–O(eq) and C–O(ax) vibrations while the E and B symmetry species refer only to C–O(eq) motion.

The two highest frequency 5-μ bands for each ion are assigned as A_1 ν(C–O) equatorial with the lower of them involving motion on the $M'(CO)_5$ moiety. This is consistent with the depolarization ratios for the $ReW(CO)_{10}^-$ compound and with the fact that the lower band shifts on going from the ReCr to the ReW ion. The vibrations at 1968 and 1939 cm^{-1} for the ReMo anion and those at 1981 and 1937 cm^{-1} for the ReW anion are assigned as B modes since they are observed only in the Raman spectra and are depolarized, as indicated by the ReW measurements. Raman spectra of the ReCr compound could not be observed above 700 cm^{-1}. The fundamentals observed at 1957 and 1963 cm^{-1} for the ReMo and ReW ions are assigned as E modes on the basis of their high infrared and low Raman intensities. The corresponding infrared vibration is located at 1965 cm^{-1} for the ReCr anion. This large intensity variation between the infrared and Raman spectra of these compounds is expected for E ν(C–O) equatorial vibrations. The lowest frequency 5-μ bands and those at *ca.* 1930 cm^{-1} are of A_1 symmetry and assigned as axial carbonyl stretches, as substantiated by polarization measurements on the ReW compound. The final CO fundamentals at 1888, 1901, and 1893 cm^{-1} for the ReCr, ReMo, and ReW anions, respectively, therefore are of E symmetry.

The complete assignment for the 5-μ fundamentals of a $M(CO)_5$ moiety for these molecules then shows the energy ordering A_1(equatorial) > B(equatorial) > E(equatorial) > A_1(axial), which is in agreement with reported assignments for $M(CO)_5X$.[15,26] The positions of the B modes in this region are readily calculable from our assigned A_1 and E stretches using approximate treatments,[27] and these are close to the assigned B frequencies.

Spectra in the Region 300–800 cm^{-1}. The ν(M–C) motions give rise to the same symmetry species (4 A_1 + 2 E + B_1 + B_2) as the ν(C–O) vibrations, and six infrared-active fundamentals (4 A_1 + 2 E) and eight Raman-active modes are expected in this region. The δ(M–C–O) vibrations are of (2 A_1 + 2 A_2 + 2 B_1 + 2 B_2 + 6 E) character with eight infrared-active (2 A_1 + 6 E) and twelve Raman-allowed fundamentals (2 A_1 + 2 B_1 + 2 B_2 + 6 E). The M–C–O deformations are equatorial in-plane (β_i), out-of-plane (β_o), or axial (β_a) type and are observed primarily in the 500–800-cm^{-1} part of this region, while ν(MC) modes dominate the lower portion (300–500 cm^{-1}). However, considerable mixing of these motions is expected.

Most of the M–C–O deformations should be strong in the infrared spectra and weak in the Raman spectra. The three highest frequency modes in this region [680, 668, and 593 cm^{-1} for ReCr; 620, 598, and 591 cm^{-1} for ReMo; and the two ReW modes at 602 and 587 cm^{-1}] are assigned as δ(M–C–O) vibrations. The highest frequency mode in each set is of A_1 symmetry and localized on the M' portion of the ion, which is consistent with its depolarization ratio in the ReW spectrum and the frequency shift on changing M' from Cr to W. The lowest frequency band for each set is also an A_1 mode associated with the Re moiety of each molecule, consistent with the polarization studies on ReW and the fact that the band position is relatively constant through the series. The third band of each set must be of E symmetry. It shifts on going from the ReCr to ReMo anion, so it is assigned to motion on the $M'(CO)_5$ moiety.

The metal–carbon stretching mode of highest frequency observed at 467, 469, and 466 cm^{-1} for the Cr, Mo, and W compounds is polarized and assigned to the Re–C(ax) A_1 vibration which is expected to be of higher frequency than the Re–C(eq) A_1 vibration. This is consistent with a previous investigation of $Re_2(CO)_{10}$.[14] The polarized band at *ca.* 430 cm^{-1} for each compound is assigned to the Re–C(eq) A_1 stretch. The lowest energy fundamental observed in this spectral region is an A_1 equatorial M'–C mode. Support for this assignment comes from the measured ρ value for the ReCr species, the shift in frequency with changing M', and the expectation that ν(M'–C) equatorial should be of lower energy than ν(M'–C) axial. The remainder of the middle-frequency bands are assigned in Table I.

Spectra in the Region below 300 cm^{-1}. There are nine allowed infrared modes (3 A_1 + 6 E) and thirteen Raman-active modes (3 A_1 + 2 B_1 + 2 B_2 + 6 E). The A_1 modes describe metal–metal stretching motion, skeletal $C–M–C^{ax}$ (Δ_a) deformations, and $M–M–C^{eq}$ (γ_e) bending motions. The B_1, B_2, and E fundamentals include $C–M–C^{eq}$ (Δ_e), Δ_a, and γ_e deformations.

The anion fundamentals, as well as certain cation vibrations and lattice and combination bands, are observed below 150

Table I. Observed and Calculated Fundamentals[a–c]

ν_i	Γ	ν_{obsd}	ν_{calcd}	ρ_{obsd}	Description
					ReCr(CO)_{10}^{-}
ν_1	A_1	2080	2080		$\nu_{\text{C-O(eq)Re}}$
ν_2	A_1	1986	1986		$\nu_{\text{C-O(eq)Cr}}$
ν_{13}	B		1981		$\nu_{\text{C-O(eq)Re}}$
ν_{20}	E	1965	1965		$\nu_{\text{C-O(eq)Re}}$
ν_{36}	B		1938		$\nu_{\text{C-O(eq)Cr}}$
ν_3	A_1	1930	1930		$\nu_{\text{C-O(ax)Re}}$
ν_{21}	E	1888	1888		$\nu_{\text{C-O(eq)Cr}}$
ν_4	A_1	1857	1857		$\nu_{\text{C-O(ax)Cr}}$
ν_5	A_1	680	680		$\delta_{\text{Cr-C-O(op)}}$
ν_{22}	E	668	667		$\delta_{\text{Cr-C-O(ax)}} + \delta_{\text{C-Cr-C(ax)}}$
ν_6	A_1	593	593	~0	$\delta_{\text{Re-C-O(op)}}$
ν_{42}	A_2		588		$\delta_{\text{Re-C-O(eq)}}$
ν_{37}	B		576		$\delta_{\text{Re-C-O(eq)}} + \delta_{\text{C-Re-C(eq)}}$
ν_{23}	E	562	564		$\delta_{\text{Re-C-O(ax)}} + \delta_{\text{C-Re-C(ax)}}$
ν_{38}	B		547		$\delta_{\text{Cr-C-O(op)}}$
ν_{24}	E		536		$\delta_{\text{Cr-C-O(eq)}} + \nu_{\text{Cr-C(eq)}}$
ν_{43}	A_2		532		$\delta_{\text{Cr-C-O(eq)}}$
ν_{15}	B		531		$\delta_{\text{Re-C-O(op)}}$
ν_{25}	E	531	530		$\delta_{\text{Re-C-O(eq)}} + \delta_{\text{C-Re-C(eq)}}$
ν_{16}	B		521		$\delta_{\text{Cr-C-O(eq)}} + \delta_{\text{C-Cr-C(eq)}}$
ν_{26}	E	478	481		$\delta_{\text{Cr-C-O(op)}} + \delta_{\text{Cr-C-O(eq)}}$
ν_{27}	E		473		$\delta_{\text{Re-C-O(op)}} + \delta_{\text{Re-C-O(ax)}}$
ν_7	A_1	467	467	~0.0	$\nu_{\text{Re-C(eq)}} + \nu_{\text{Re-C(ax)}}$
ν_{28}	E	457	456		$\nu_{\text{Cr-C(eq)}} + \delta_{\text{Cr-C-O(ax)}}$
ν_8	A_1	439	438		$\nu_{\text{Cr-C(ax)}}$
ν_9	A_1	427	426	0.0	$\nu_{\text{Re-C(ax)}} + \nu_{\text{Re-C(eq)}}$
ν_{29}	E	419	419	0.85	$\nu_{\text{Re-C(eq)}}$
ν_{10}	A_1	408	406	0.08	$\nu_{\text{Cr-C(eq)}}$
ν_{17}	B	379			$\nu_{\text{Re-C(eq)}}$
ν_{39}	B	349			$\nu_{\text{Cr-C(eq)}}$
ν_{11}	A_1	146	146	0.24	$\nu_{\text{Re-Cr}} + \delta_{\text{C-Cr-C(ax)}}$
ν_{30}	E		126		$\delta_{\text{C-Cr-C(ax)}} + \delta_{\text{C-Cr-C(eq)}}$
ν_{31}	E		119		$\delta_{\text{C-Re-C(ax)}} + \delta_{\text{C-Cr-C(ax)}}$
ν_{12}	B		112		$\delta_{\text{C-Re-C(eq)}} + \delta_{\text{Re-C-O(eq)}}$
ν_{18}	B		107		$\delta_{\text{C-Cr-C(eq)}} + \delta_{\text{Cr-C-O(eq)}}$
ν_{32}	E		96		$\delta_{\text{C-Cr-C(eq)}} + \delta_{\text{C-Re-C(eq)}}$
ν_{19}	B		93		$\delta_{\text{C-Re-C(ax)}} + \delta_{\text{Cr-Re-C(eq)}}$
ν_{33}	E		90		$\delta_{\text{C-Re-C(eq)}} + \delta_{\text{C-Cr-C(eq)}}$
ν_{41}	B		69		$\delta_{\text{C-Cr-C(ax)}} + \delta_{\text{Cr-C-O(op)}}$
ν_{34}	E		66		$\delta_{\text{Cr-Re-C(eq)}} + \delta_{\text{C-Cr-C(eq)}}$
ν_{13}	A_1		50		$\delta_{\text{C-Cr-C(ax)}} + \delta_{\text{Cr-Re-C(eq)}}$
ν_{35}	E		27		$\delta_{\text{Re-Cr-C(eq)}} + \delta_{\text{Cr-C-O(op)}}$
					$\lvert\sum_{i=1}^{\alpha}\nu(\text{calcd}) - \nu(\text{obsd})\rvert/\alpha = 0.8\ \text{cm}^{-1}$
					ReMo(CO)_{10}^{-}
ν_1	A_1	2075	2075		$\nu_{\text{C-O(eq)Re}}$
ν_2	A_1	2009	2009		$\nu_{\text{C-O(eq)Mo}}$
ν_1	A_1	2075	2075		$\nu_{\text{C-O(eq)Re}}$
ν_2	A_1	2009	2009		$\nu_{\text{C-O(eq)Mo}}$
ν_{14}	B	1968	1968		$\nu_{\text{C-O(eq)Re}}$
ν_{20}	E	1957	1957		$\nu_{\text{C-O(eq)Re}}$
ν_{36}	B	1939	1939		$\nu_{\text{C-O(eq)Mo}}$
ν_3	A_1	1925	1925		$\nu_{\text{C-O(ax)Re}}$
ν_{21}	E	1901	1901		$\nu_{\text{C-O(eq)Mo}}$
ν_4	A_1	1861	1861		$\nu_{\text{C-O(ax)Mo}}$
ν_5	A_1	620	620		$\delta_{\text{Mo-C-O(op)}}$
ν_{22}	E	598	599		$\delta_{\text{Mo-C-O(ax)}} + \delta_{\text{C-Mo-C(ax)}}$
ν_6	A_1	591	591		$\delta_{\text{Re-C-O(op)}}$
ν_{42}	A_2		588		$\delta_{\text{Re-C-O(eq)}}$
ν_{37}	B		576		$\delta_{\text{Re-C-O(eq)}} + \delta_{\text{C-Re-C(eq)}}$
ν_{23}	E	564	564		$\delta_{\text{Re-C-O(ax)}} + \delta_{\text{C-Re-C(ax)}}$
ν_{43}	A_2		538		$\delta_{\text{Mo-C-O(eq)}}$
ν_{15}	B		531		$\delta_{\text{Re-C-O(op)}}$
ν_{24}	E	529	530		$\delta_{\text{Re-C-O(eq)}}$
ν_{38}	B		529		$\delta_{\text{Mo-C-O(op)}}$
ν_{16}	B		524		$\delta_{\text{Mo-C-O(eq)}} + \delta_{\text{C-Mo-C(eq)}}$
ν_{25}	E	508	508		$\delta_{\text{Mo-C-O(eq)}} + \delta_{\text{C-Mo-C(eq)}}$
ν_{26}	E		486		$\delta_{\text{Mo-C-O(op)}} + \delta_{\text{Mo-C-O(ax)}}$
ν_{27}	E		473		$\delta_{\text{Re-C-O(op)}} + \delta_{\text{Re-C-O(ax)}}$
ν_7	A_1	469	467		$\nu_{\text{Re-C(eq)}} + \nu_{\text{Re-C(ax)}}$
ν_8	A_1	428	426		$\nu_{\text{Re-C(ax)}} + \nu_{\text{Re-C(eq)}}$
ν_{28}	E	419	422		$\nu_{\text{Re-C(eq)}}$
ν_9	A_1	416	416		$\nu_{\text{Mo-C(ax)}} + \nu_{\text{Mo-C(eq)}}$
ν_{29}	E	406	406		$\nu_{\text{Mo-C(eq)}}$
ν_{10}	A_1	387	387		$\nu_{\text{Mo-C(eq)}} + \nu_{\text{Mo-C(ax)}}$
ν_{17}	B		385		$\nu_{\text{Re-C(eq)}}$
ν_{39}	B		353		$\nu_{\text{Mo-C(eq)}}$
ν_{11}	A_1	130	130		$\nu_{\text{Re-Mo}} + \delta_{\text{C-Mo-C(ax)}}$
ν_{30}	E		120		$\delta_{\text{C-Re-C(ax)}} + \delta_{\text{C-Mo-C(ax)}}$
ν_{31}	E		116		$\delta_{\text{C-Mo-C(ax)}} + \delta_{\text{C-Re-C(ax)}}$
ν_{40}	B		112		$\delta_{\text{C-Re-C(eq)}} + \delta_{\text{Re-C-O(eq)}}$
ν_{18}	B		110		$\delta_{\text{C-Mo-C(eq)}} + \delta_{\text{Mo-C-O(eq)}}$
ν_{12}	A_1	110	109		$\delta_{\text{C-Re-C(ax)}} + \delta_{\text{Mo-Re-C(eq)}}$
ν_{32}	E		94		$\delta_{\text{C-Mo-C(eq)}} + \delta_{\text{C-Re-C(eq)}}$
ν_{33}	E		90		$\delta_{\text{C-Re-C(eq)}} + \delta_{\text{C-Mo-C(eq)}}$
ν_{19}	B		88		$\delta_{\text{C-Re-C(ax)}} + \delta_{\text{Mo-Re-C(eq)}}$
ν_{41}	B		71		$\delta_{\text{C-Mo-C(ax)}} + \delta_{\text{Re-Mo-C(eq)}}$
ν_{34}	E		59		$\delta_{\text{Mo-Re-C(eq)}}$
ν_{13}	A_1		48		$\delta_{\text{C-Mo-C(ax)}} + \delta_{\text{C-Re-C(ax)}}$
ν_{35}	E		30		$\delta_{\text{Re-Mo-C(eq)}}$
					$\lvert\sum_{i=1}^{\alpha}\nu(\text{calcd}) - \nu(\text{obsd})\rvert/\alpha = 0.5\ \text{cm}^{-1}$
					ReW(CO)_{10}^{-}
ν_1	A_1	2079	2079	0.12	$\nu_{\text{C-O(eq)Re}}$
ν_2	A_1	2011	2011	0.22	$\nu_{\text{C-O(eq)W}}$
ν_{14}	B	1981	1981	0.90	$\nu_{\text{C-O(eq)Re}}$
ν_{20}	E	1963	1963		$\nu_{\text{C-O(eq)Re}}$
ν_{36}	B	1937	1937	0.76	$\nu_{\text{C-O(eq)W}}$
ν_3	A_1	1929	1929	0.75	$\nu_{\text{C-O(ax)Re}}$
ν_{21}	E	1893	1893		$\nu_{\text{C-O(eq)W}}$
ν_4	A_1	1857	1857		$\nu_{\text{C-O(ax)W}}$
ν_5	A_1	602	602	0.25	$\delta_{\text{W-C-O(op)}} + \delta_{\text{Re-C-O(op)}}$
ν_{42}	A_2		588		$\delta_{\text{Re-C-O(eq)}}$
ν_6	A_1	587	585	0.40	$\delta_{\text{Re-C-O(op)}} + \delta_{\text{W-C-O(op)}}$
ν_{37}	B		576		$\delta_{\text{Re-C-O(eq)}} + \delta_{\text{C-Re-C(eq)}}$
ν_{22}	E		575		$\delta_{\text{W-C-O(ax)}} + \delta_{\text{C-W-C(ax)}}$
ν_{23}	E		564		$\delta_{\text{Re-C-O(ax)}} + \delta_{\text{C-Re-C(ax)}}$
ν_{43}	A_2		563		$\delta_{\text{W-C-O(eq)}}$
ν_{15}	B		549		$\delta_{\text{W-C-O(eq)}} + \delta_{\text{C-W-C(eq)}}$
ν_{16}	B		533		$\delta_{\text{Re-C-O(op)}}$
ν_{24}	E		530		$\delta_{\text{W-C-O(eq)}}$
ν_{25}	E	529	529	0.90	$\delta_{\text{Re-C-O(eq)}}$
ν_{38}	B		509		$\delta_{\text{W-C-O(op)}}$
ν_{26}	E		473		$\delta_{\text{Re-C-O(op)}} + \delta_{\text{Re-C-O(ax)}}$
ν_{27}	E		471		$\delta_{\text{W-C-O(op)}} + \delta_{\text{W-C-O(ax)}}$
ν_7	A_1	466	463	0.0	$\nu_{\text{Re-C(eq)}} + \nu_{\text{Re-C(ax)}}$
ν_8	A_1	441	441	0.03	$\nu_{\text{W-C(ax)}} + \nu_{\text{W-C(eq)}}$
ν_9	A_1	434	429		$\nu_{\text{Re-C(ax)}} + \nu_{\text{Re-C(eq)}}$
ν_{28}	E	415	415	0.75	$\nu_{\text{W-C(eq)}}$
ν_{29}	E	393	393	0.81	$\nu_{\text{Re-C(eq)}}$
ν_{10}	A_1		391		$\nu_{\text{W-C(eq)}} + \nu_{\text{W-C(ax)}}$
ν_{17}	B		379		$\nu_{\text{Re-C(eq)}}$
ν_{39}	B		378		$\nu_{\text{W-C(eq)}}$
ν_{30}	E		118		$\delta_{\text{C-Re-C(ax)}} + \delta_{\text{Re-C-O(ax)}}$
ν_{11}	A_1	109	112		$\nu_{\text{Re-W}} + \delta_{\text{C-Re-C(ax)}}$
ν_{40}	B		112		$\delta_{\text{C-Re-C(eq)}} + \delta_{\text{Re-C-O(eq)}}$
ν_{18}	B		111		$\delta_{\text{C-W-C(eq)}} + \delta_{\text{W-C-O(eq)}}$
ν_{31}	E		105		$\delta_{\text{C-W-C(ax)}}$
ν_{12}	A_1		96		$\delta_{\text{C-W-C(ax)}} + \delta_{\text{C-Re-C(ax)}}$
ν_{32}	E		90		$\delta_{\text{C-Re-C(eq)}} + \delta_{\text{C-W-C(eq)}}$
ν_{33}	E		88		$\delta_{\text{C-W-C(eq)}} + \delta_{\text{C-Re-C(eq)}}$
ν_{19}	B		86		$\delta_{\text{C-Re-C(ax)}} + \delta_{\text{W-Re-C(eq)}}$
ν_{41}	B		67		$\delta_{\text{C-W-C(ax)}} + \delta_{\text{Re-W-C(eq)}}$
ν_{34}	E		42		$\delta_{\text{W-Re-C(eq)}} + \delta_{\text{Re-W-C(eq)}}$
ν_{13}	A_1		37		$\delta_{\text{C-W-C(ax)}} + \delta_{\text{C-Re-C(ax)}}$
ν_{35}	E		28		$\delta_{\text{Re-W-C(eq)}} + \delta_{\text{W-Re-C(eq)}}$
					$\lvert\sum_{i=1}^{\alpha}\nu(\text{calcd}) - \nu(\text{obsd})\rvert/\alpha = 0.8\ \text{cm}^{-1}$

[a] The inactive A_2 torsion mode was not included in these calculations. [b] All observed band positions are reported for solution spectra except where bands were observed only in the solid state. Frequencies are given in cm^{-1}. [c] Abbreviations used: eq, equatorial; ax, axial; op, out of the equatorial plane.

Table II. Ultraviolet-Visible Band Maxima of $ReM'(CO)_{10}^-$ Anions in Tetrahydrofuran Solution (25,000-35,000 cm^{-1})[a]

Compd	Band I	Band II	Compd	Band I	Band II
$Et_4NReCr(CO)_{10}$	25,500	31,400	$Et_4NReW(CO)_{10}$	27,300	33,000
$Et_4NReMo(CO)_{10}$	27,400	32,500	$Ph_4AsReW(CO)_{10}$	27,300	32,700

[a] Quartz cells of 1-cm path length were used.

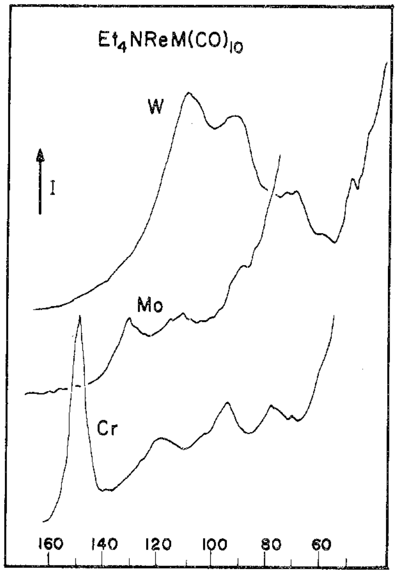

Figure 1. Raman spectra (50-175 cm^{-1}) of solid $Et_4NReM(CO)_{10}$ compounds: W, $Et_4NReW(CO)_{10}$; Mo, $Et_4NReMo(CO)_{10}$; Cr, $Et_4NReCr(CO)_{10}$, each taken with 632.8-nm excitation. Spectra are offset arbitrarily for clarity of display.

cm^{-1}. Solution spectra were measured with the hope of reducing or eliminating the complications which arise from solid-state effects, but they were of little use because there are still broad overlapping bands in this narrow region, so the assignments here rest primarily on the solid-state spectra.

The Raman band at 146 cm^{-1} for $ReCr(CO)_{10}^-$ in solution is assigned as the A_1 metal-metal stretching mode, since it is very intense and polarized. The corresponding fundamental for the ReMo molecule was located at 130 cm^{-1}, but a ν(Re-W) band clearly separate from the absorptions for other skeletal deformations was not observable. Those vibrations observed at 117, 110, and 109 cm^{-1} for the ReCr, ReMo, and ReW anions, respectively, are due largely to A_1 deformations involving Δ_a bending motion in the ReCr and ReMo cases but are due to both of them and ν(Re-W) in the ReW case. Vibrational fundamentals at *ca.* 90 cm^{-1} and between 70 and 80 cm^{-1} are of either E or B symmetry. The 90-cm^{-1} bands are associated with Δ_e or Δ_a deformations while the lower frequency modes are assumed to be primarily comprised of M-M-C^{eq} (γ_e) bending motion.

For $ReW(CO)_{10}^-$, ν(ReW) is expected at lower than 122 cm^{-1}, the frequency to which ν(ReRe) in $Re_2(CO)_{10}$ is commonly assigned.[3] The most intense low-frequency Raman band of $ReW(CO)_{10}^-$ is centered at *ca.* 110 cm^{-1}. As shown in Figure 1, it is somewhat broadened to the high-frequency side and strongly overlapped with other bands to the low-frequency side and is much stronger relative to the lower frequency deformation modes than are the 117- and 110-cm^{-1} modes for the ReCr and ReMo ions. All of these facts point to the occurrence of the predominantly ν(ReW) mode at *ca.* 110 cm^{-1}, adding intensity to the deformation band manifold in this region. Accordingly, we assign ν(ReW) the value of *ca.* 110 cm^{-1}, with an uncertainty of perhaps 3 cm^{-1}, which is more likely to the high-frequency side. Attempts to enhance this band resonantly relative to others have failed to produce significant differentiation, presumably because the A_1 "umbrella-type" motions involving Δ_a mix most strongly with ν(MM) in general and ν(ReW) in particular. The sought-for enhancement would have been *via* off-resonance (preresonance) interaction with the $A_1 \rightarrow B_2$ (σ(Re-W) $\rightarrow$ σ^*(Re-W)) band centered at 33 kK.

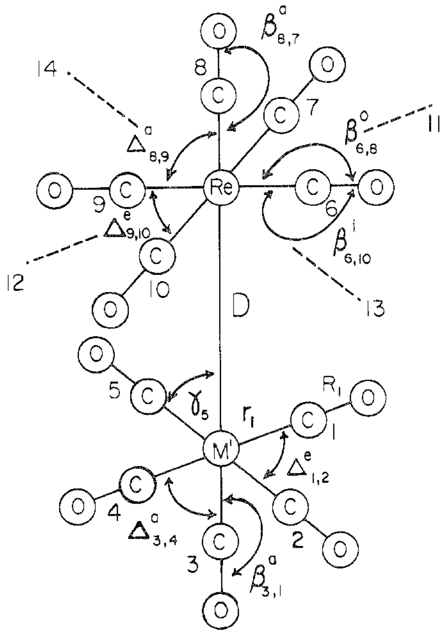

Figure 2. Idealized molecular geometry of the $ReM'(CO)_{10}^-$ anions (C_{4v}) including internal valence coordinates, defined as follows: $R_j = C_j$–O; $r_j = C_j$–M; $\beta_{j,k} = \delta$(M–C_j–O) in the C_j–M–C_k plane with C_j displaced toward k in $+\beta_{j,k}$; $\Delta^e_{j,k} = \delta(C_j$–M–$C_k)$ with both carbon atoms in the equatorial carbonyl plane, positive when opening; $\gamma_j = \delta$(M–M–C_j) where C_j is an equatorial carbon atom, positive when opening; $\Delta^a_{j,k} = \delta(C_j$–M–$C_k)$ where one carbon is axial, along the C_4 axis, and one is equatorial, positive when opening.

Visible-Near-Uv Spectra. The visible-ultraviolet spectra of the $ReM'(CO)_{10}^-$ anions contain the two principal absorptions reported in Table II. By analogy to the spectra of the neutral decacarbonyls $M_2(CO)_{10}$ (M = Mn, Tc, Re)[28] and the anions $MnM'(CO)_{10}^-$ (M = Cr, Mo, W),[2] the higher frequency, more intense band in these anions is assigned to the [dσ(M-M') $\rightarrow$ dσ^*(M-M')] transition, which involves the metal-metal σ-bonding molecular orbital and its corresponding antibonding orbital. The order of the energies of this transition is Re-W > Re-Mo > Re-Cr.

The lower frequency transition is assigned to the transition which involves the d_π MO's of each $M(CO)_5$ unit and the σ^*(M-M') MO and is represented conveniently as a $d_\pi \rightarrow \sigma^*$(MM') transition.

Vibrational Analysis. Normal-coordinate analyses were performed for the $ReM'(CO)_{10}^-$ species to obtain values for k(Re-M') and information about the forms of the normal vibrations involving the metal-metal bonds. In the analyses of these large molecules, as for the $MnM'(CO)_{10}^-$ anions, it is not possible to obtain a complete or unique force field for each compound, of course. However, it is possible to obtain key force constants from calculations constrained by the requirements that the entire observed spectrum be fit closely by the calculated frequencies and that the eigenvector representations of the calculated frequencies agree with the spectral assignments.

The symmetry coordinates employed in these calculations[29]

Table III. Nonzero Force Field Elements for the $ReM'(CO)_{10}^-$ Species

A. Force Field Elements[a,b,c,f] Constant through the Series

β_a	0.32	r_a	2.87	Δ_a'',Δ_a''(trans)	−0.01
β_i	0.35	r'',R''	0.735[e]	Δ_a'',Δ_a''(cis)	−0.01
β_o'',β_o''(trans)	0.04	r_a'',D	0.10	γ_e,γ_e'(cis)	−0.013[d]
β_i,β_i(trans)	0.04	Δ_e''	0.10	γ_e,γ_e'(trans)	−0.013[d]
β_i'',β_i''(cis)	0.02	r_a,β_o	−0.065	r_e',Δ_e'(cis)	0.03[e]
β_i',β_i'(trans)	0.02	Δ_a	0.15	r_e,β_a	0.014
β_o,β_o(cis)	0.02	Δ_e'',Δ_e''(trans)	−0.01	r_e',Δ_e'(trans)	−0.03
γ_e'	0.02	Δ_e'',Δ_e''(cis)	−0.01	r_a,γ_e	0.05
R_e,R_a(cis)	0.28	β_a,β_o	0.014		

B. Force Fields[a,b,c,f] Varied through the Series

	ReCr-$(CO)_{10}^-$	ReMo-$(CO)_{10}^-$	ReW-$(CO)_{10}^-$		ReCr-$(CO)_{10}^-$	ReMo-$(CO)_{10}^-$	ReW-$(CO)_{10}^-$
r_e	2.60	2.64	2.64	r_e'	2.20	2.08	2.44
r_a'	2.21	2.17	2.58	β_a'	0.43	0.37	0.35
R_e	16.05	15.91	16.09	R_e'	15.06	15.29	15.09
R_a	15.13	15.05	15.10	R_a'	14.14	14.24	14.10
D	0.67	0.72	0.74	β_i'	0.30	0.30	0.33
β_o	0.31	0.31	0.32	β_o'	0.35	0.33	0.32
γ_e	0.095	0.07	0.03	Δ_a'	0.14	0.12	0.10
r_e,r_e(cis)	0.25	0.23	0.25	r_e',r_e'(cis)	0.19	0.15	0.13
r_e,r_a(cis)	0.15	0.15	0.13	r_e',r_a'(cis)	0.04	0.09	0.17
r_e,r_e(trans)	0.30	0.30	0.45	r_e',r_e'(trans)	0.20	0.28	0.20
R_e,R_e(cis)	0.27	0.31	0.27	R_e',R_e'(cis)	0.10	0.20	0.20
R_e,R_e(trans)	0.38	0.37	0.35	R_e',R_e'(trans)	0.48	0.45	0.52
R_e',R_a'	0.21	0.23	0.27	β_o',γ_e'[e]	0.03	0.00	0.00
β_o',β_o'(cis)	0.03	0.025	0.025	β_a',β_o'	0.06	0.02	0.02

[a] All force field elements are in millidynes per angstrom. [b] All internal valence coordinates are defined as positive for bond stretching or angle opening; thus all force field elements have unique signs. [c] Primed and nonprimed valence force constants refer to the M' and Re ends of the molecules, respectively, whereas double-primed force constants are equivalent for both halves of a molecule. [d] The cis and trans designations of these valence force constants refer to the projection of the M–C bond of either γ_e or γ_e' onto the carbonyl plane of the opposite half of the molecule. In the cis notation there is 45° between the M–C projection of γ_e and the M–C of γ_e' whereas in the trans there is 135°. [e] These internal coordinates share a common carbon. [f] Some force field elements in this table have been rounded off for presentation. The precise final values used in the normal-coordinate analyses may be obtained by writing to the authors.

were obtained from a set of internal valence coordinates, based on the definitions of Figure 2, and the force constants reported in Table III are defined in terms of these coordinates. The eigenvalue calculations were carried out with the GMAT and VSEC programs of Schachtschneider.[30]

The criteria employed in refining the fields were the closeness of fit between the calculated and observed frequencies and the accuracy of the calculated eigenvector representation of the motions assigned to the vibrational bands. Other criteria, based on the spectral similarities between the individual $ReM'(CO)_{10}^-$ anions and between them and analogous $MnM'(CO)_{10}^-$ species, are that the portion of the force fields proper to the $Re(CO)_5$ moiety be essentially the same for each Re species and that those pertaining to the $M'(CO)_5$ unit of a Mn or Re compound, for the same M', be similar. These are useful criteria since they constrain the ranges of force constant values. The final constraint is that the force fields be as small as is consistent with retaining force constants whose values must be appreciably different from zero.[31]

The starting force constants for the $M'(CO)_5$-based coordinates were transferred from the corresponding group of the $MnM'(CO)_{10}^-$ species, and those for the $Re(CO)_5$-based coordinates were obtained from investigations of $Re(CO)_5X$ and $Re_2(CO)_{10}$ species.[3,8–9,27] Initial values for k(Re–M') were estimated from ν(Re–M') using a factored vibrational analysis including the atoms on the C_4 axis, and the k(CO)'s were estimated from an energy-factored analysis of the ν(CO) spectra.

The results of the calculations and a comparison of observed and calculated frequencies are listed in Table I. The closeness of fit, defined as ϵ, where $\epsilon = [\sum_i|\nu_i(\text{calcd}) - \nu_i(\text{obsd})|]/\alpha$, is 2 cm^{-1} or less in each case, so further refinement is not justified.

Discussion

The bond strength information provided by the k(Re–M) values permits comparison of metal–metal bonds in the closely related compounds of the several $MM'(CO)_{10}$ series. Although the three k(Re–M) values in the $ReM(CO)_{10}^-$ set are close, they fall in the order k(Re–W) > k(Re–Mo) > k(Re–Cr). This order is analogous to that for the related $MnM(CO)_{10}^-$ set, k(Mn–W) > k(Mn–Mo) > k(Mn–Cr), and makes clear that in these homologous series bonding to the $W(CO)_5$ moiety is stronger than that to the $Cr(CO)_5$ moiety. As discussed earlier,[2] this primarily reflects the higher overlap achieved by Mn or Re bonding to W compared to that with Cr. This is also reflected in the fact that the bond strength for each $MnM(CO)_{10}^-$ compound is lower than for the analogous $ReM(CO)_{10}^-$ compounds. Thus, k(Re–Cr) > k(Mn–Cr); k(Re–Mo) > k(Mn–Mo); and k(Re–W) > k(Mn–W).

Among isoelectronic sets of molecules of the $MM'(CO)_{10}$ form, the neutral species have the highest metal–metal bond strengths. Thus, k(Mn–Re) > k(Mn–W) > k(Re–Cr); k(Re–Re) > k(Re–W); and k(Mn–Mn) > k(Mn–Cr). The basis metal orbitals of the neutral species, such as $ReMn(CO)_{10}$, are expected to have essentially the same extension as those of the isoelectronic mononegative species, $ReCr(CO)_{10}^-$ in this case, so the degree of metal–metal (d_{z^2}) overlap should be nearly the same in two analogous species. However, the varied metal atom has a higher nuclear charge, and thus lower orbital energies, in the neutral species, so a stronger bond is expected.

Throughout the group of $MM'(CO)_{10}$ compounds, the metal–metal bond strengths indicate single-bond formation with subtle variations which reflect metal orbital extension changes and the distribution of nuclear charge in isoelectronic and homologous series.

Acknowledgment. We gratefully acknowledge support of this work under the Materials Science Program of Brown University with contract support by the Advanced Research Projects Agency (SD-86) and the National Science Foundation. A NASA fellowship to J.R.J. is gratefully acknowledged. The laser Raman instrument purchase was made possible in part through Grant GP-10187 from the National Science Foundation. The assistance of Mr. Wayne M. Butler and Dr. Robert J. Ziegler is gratefully acknowledged.

Registry No. $Et_4NReCr(CO)_{10}$, 54307-62-9; $Et_4NReMo(CO)_{10}$, 54307-63-0; $Et_4NReW(CO)_{10}$, 54307-64-1; $Ph_4AsReW(CO)_{10}$, 54307-65-2.

Supplementary Material Available. Table IV, an extensive listing of all observed infrared and Raman bands including their intensities, physical states during measurement, polarizations, and assignments, will appear following these pages in the microfilm edition of this volume of the journal. Photocopies of the supplementary material from this paper only or microfiche (105 × 148 mm, 24× reduction, negatives) containing all of the supplementary material for the papers in this issue may be obtained from the Journals Department, American Chemical Society, 1155 16th St., N.W., Washington, D.C. 20036. Remit check or money order for $4.00 for photocopy or $2.50 for microfiche, referring to code number AIC40691M.

References and Notes

(1) Abstracted in part from the Ph.D. thesis of J. R. Johnson, Brown University, 1973.
(2) J. R. Johnson, R. J. Ziegler, and W. M. Risen, Jr., *Inorg. Chem.*, **12**, 2349 (1973).
(3) C. O. Quicksall and T. G. Spiro, *Inorg. Chem.*, **8**, 2363 (1969).
(4) G. O. Evans, W. T. Wozniak, and R. K. Sheline, *Inorg. Chem.*, **9**, 979 (1970).
(5) M. A. Bennett and R. J. H. Clark, *J. Chem. Soc.*, 5560 (1964).
(6) I. J. Hyams, D. Jones, and E. R. Lippincott, *J. Chem. Soc. A*, 1987 (1967).
(7) A. Davison and J. W. Faller, *Inorg. Chem.*, **6**, 845 (1967).
(8) N. Flitcroft, D. K. Huggins, and H. D. Kaesz, *Inorg. Chem.*, **3**, 1123 (1964).
(9) F. A. Cotton and R. M. Wing, *Inorg. Chem.*, **4**, 1328 (1965).
(10) D. J. Parker and M. H. B. Stiddard, *J. Chem. Soc. A*, 695 (1966).
(11) H. M. Gager, J. Lewis, and M. J. Ware, *Chem. Commun.*, 616 (1966).
(12) D. M. Adams and A. Squire, *J. Chem. Soc. A*, 2817 (1968).
(13) D. M. Adams, M. A. Hooper, and A. Squire, *Chem. Commun.*, 1188 (1970).
(14) D. M. Adams, M. A. Hooper, and A. Squire, *J. Chem. Soc. A*, 71 (1971).
(15) R. J. H. Clark and B. C. Crosse, *J. Chem. Soc. A*, 224 (1969).
(16) U. Anders and W. A. G. Graham, *J. Amer. Chem. Soc.*, **89**, 539 (1967).
(17) Calibration in the 33–600-cm^{-1} region was performed with the results of L. R. Blaine, *J. Res. Nat. Bur. Stand., Sect. C*, **67**, 207 (1963), and L. R. Blaine, E. K. Plyler, and W. S. Benedict, *J. Res. Nat. Bur. Stand., Sect. A*, **66**, 223 (1962). For the region 600–2500 cm^{-1} see "Tables of Wavenumbers for the Calibration of Spectrometers," IUPAC Commission on Molecular Spectroscopy, Butterworths, London, 1961.
(18) L. F. Dahl, E. Ishishi, and R. E. Rundle, *J. Chem. Phys.*, **26**, 1750 (1957).
(19) L. F. Dahl and R. E. Rundle, *Acta Crystallogr.*, **16**, 419 (1963).
(20) M. F. Bailey and L. F. Dahl, *Inorg. Chem.*, **4**, 1140 (1965).
(21) L. B. Handy, J. K. Ruff, and L. F. Dahl, *J. Amer. Chem. Soc.*, **92**, 7312 (1970).
(22) For conciseness, the following abbreviations will be used in the text, where feasible, ReW for $ReW(CO)_{10}^-$, ReMo for $ReMo(CO)_{10}^-$, and ReCr for $ReCr(CO)_{10}^-$ and their Et_4N^+ and Ph_4As^+ salts.
(23) A. Whitaker and J. W. Jeffery, *Acta Crystallogr.*, **23**, 977 (1967).
(24) S. P. Arnesen and H. M. Seip, *Acta Chem. Scand.*, **29**, 2711 (1966).
(25) Supplementary material.
(26) I. S. Butler and H. K. Spendjian, *Can. J. Chem.*, **47**, 4117 (1969).
(27) F. A. Cotton and C. S. Kraihanzel, *J. Amer. Chem. Soc.*, **84**, 4432 (1962).
(28) R. A. Levenson, H. B. Gray, and G. P. Ceasar, *J. Amer. Chem. Soc.*, **92**, 3653 (1970).
(29) Table VII of ref 2.
(30) J. H. Schachtschneider, Technical Reports No. 231-64 and 57-65, Shell Development Co., Emeryville, Calif., 1964 and 1965.
(31) We estimate that within these constraints the values of $k(M-M')$ could be varied by ±0.01 mdyn/Å without causing significant perturbations to parts of the individual force fields which are now held constant for all members of the series.

Contribution from the Department of Chemistry,
Cornell University, Ithaca, New York 14850

Bonding Capabilities of Transition Metal Carbonyl Fragments

MIHAI ELIAN and ROALD HOFFMANN*

Received December 4, 1974 AIC40811Q

The energy ordering, symmetry, and extent in space of the valence molecular orbitals of a range of geometries of $M(CO)_3$, $M(CO)_4$, and $M(CO)_5$ fragments, where M is a transition metal center, are analyzed in detail. The properties of the fragment orbitals are then used to examine the ability of the fragments to interact with other ligands as well as the geometrical preferences of the isolated fragments. The following problems are discussed: the pyramidality of five-coordinate fragments, metal–metal bond formation, seven-coordination, stabilization of "umbrella" distortions of fragments, the difference between $M(CO)_n$ fragments and ML_n, with $L = \pi$ donor, geometrical distortions in transition metal hydrides, why $Fe(CO)_3$ favors bonding with conjugated dienes while $Cr(CO)_4$ coordinates preferentially with unconjugated dienes.

The usual contemporary way of analyzing the electronic structure of a chemical compound is in terms of molecular orbitals formed as linear combinations of atomic orbitals. For complex molecules of low symmetry these molecular orbitals can be quite delocalized. The practicing chemist, wishing to perceive the main features of the bonding and their chemical consequences, faces the sometimes difficult task of translating the information hidden in the delocalized, complicated wave function, into less exact qualitative concepts.

An alternative approach, designed to bridge the gap between the delocalized molecular orbital and the localized semantic structure of the experimentalist, consists of breaking up the molecule into fragments rather than atoms. The orbitals of the simple fragments are easily visualized. The initial bonding follows from the interaction of a limited subset of fragment orbitals, such as the highest occupied molecular orbital (HOMO) and the lowest unoccupied MO (LUMO), the valence or frontier orbitals of the fragments. Fragment analysis has been successfully used for some time for small and organic molecules.[1-3]

For transition metal complexes nothing seems more natural today than the partitioning into metal and ligand orbitals. Yet the decomposition of a complex into an invariant fragment ML_n, consisting of a metal atom and several ligands, and a variable ligand L' has not been sufficiently exploited.[4] The purpose of this paper is to demonstrate that a consistent analysis of ML_n fragments may be successfully applied to a wide range of structural problems.

The subject of our study is the set of $M(CO)_n$ fragments with $n = 3–5$ and M a metal atom of any transition series. The d-electron configuration is a variable. The specific calculations carried out were of the extended Hückel type, for M = Mn. Details are given in the Appendix. Since many of the conclusions we draw are based on symmetry arguments abstracted from the calculations, our results should carry over to any transition metal center. Our initial hope was that the con-